MR imaging and CT in three cases of Sturge-Weber syndrome: prospective comparison.

M C Chamberlain, G A Press and J R Hesselink

AJNR Am J Neuroradiol 1989, 10 (3) 491-496
http://www.ajnr.org/content/10/3/491

MR Imaging and CT in Three Cases of Sturge-Weber Syndrome: Prospective Comparison

Marc C. Chamberlain[1]
Gary A. Press[2]
John R. Hesselink[2]

Three patients with Sturge-Weber syndrome (5 months, 6 years, and 17 years old) were studied prospectively with MR imaging and CT of the brain. Both techniques demonstrated parenchymal volume loss, choroid plexus enlargement, calvarial hemiatrophy, and proptosis. In regions of parenchymal volume loss, MR alone demonstrated thickened cortex with decreased convolutions and abnormal white matter. A focal thalamic lesion and prominent medullary and subependymal veins were also shown better by MR. However, CT definitively demonstrated the characteristic cortical calcification, while T2-weighted MR images detected only smaller, nonspecific foci of hypointense signal.

MR and CT are complementary in the evaluation of Sturge-Weber syndrome.

The Sturge-Weber syndrome is a phakomatosis that includes the following clinical characteristics: a facial vascular nevus in the territory of the ophthalmic division of the trigeminal nerve, seizures, dementia, hemiplegia, hemianopsia, and buphthalmos or glaucoma. Intraparenchymal calcification, parenchymal volume loss, engorgement of deep veins, and leptomeningeal and choroid plexus angiomata may be demonstrated by neuroradiologic studies including skull films, angiography, and CT [1–8]. Descriptions of the MR findings in this disorder are limited [7, 9]. We compared 1.5-T MR and CT of the CNS in three pediatric patients with Sturge-Weber syndrome.

Subjects and Methods

Informed consent was obtained from the parents or guardians of the children who served as subjects of this investigation and, when appropriate, from the subjects themselves. The one female and two male subjects were 5 months, 6 years, and 17 years old at the time of scanning.

MR of the entire brain was performed with a 1.5-T superconducting magnet.* With a spin-echo pulse sequence, axial T2-weighted, 3000/70 (TR/TE), and proton-density-weighted, 3000/25, images were acquired in every patient. Sagittal and coronal T1-weighted, 600/25, images were obtained in two patients (cases 1 and 2). The slice thickness was 5 mm with a 2.5-mm interval between successive slices in all instances. A 256 × 256 matrix was used in all examinations.

All head CT scans were obtained on a GE 9800 scanner.* Contiguous 10-mm-thick axial sections were obtained from the foramen magnum to the vertex both before and after administration of IV contrast medium.†

MR and CT were performed prospectively and viewed independently of one another by two neuroradiologists blinded to clinical data. The examinations were assessed for evidence of atrophy (noted as dilatation of sulci and/or ventricles), abnormality of the gray or white matter, parenchymal calcification, and choroid plexus or other deep or superficial vascular anomaly. Subsequently, the MR and CT examinations of each patient were viewed simultaneously to compare the ability of each test to depict the various manifestations of Sturge-Weber syndrome.

* General Electric, Milwaukee, WI.
† Conray 60, Mallinckrodt, Inc., St. Louis, MO.

Received March 21, 1988; accepted after revision September 9, 1988.

[1] Department of Neurosciences, University of California, San Diego, School of Medicine, 225 Dickinson St., San Diego, CA 92103. Address reprint requests to M. C. Chamberlain.

[2] Department of Radiology and Magnetic Resonance Institute, University of California, San Diego, School of Medicine, San Diego, CA 92103.

AJNR **10:491–496, May/June 1989**
0195–6108/89/1003–0491

Results

Table 1 lists the clinical history and findings on physical examination in the three patients with Sturge-Weber syndrome; the results of the imaging studies are summarized in Table 2.

Asymmetric, bilateral CNS parenchymal volume loss was detected in two patients (cases 1 and 2). Dilatation of sulci and ventricular CSF spaces was most evident in the left frontal and right parietal regions in case 1 (Figs. 1A and 1B); left frontal and left parietal atrophy were predominant in case 2 (Fig. 2). In case 3, a patient with unilateral CNS atrophy, all lobes were affected. MR and CT demonstrated the regions of parenchymal atrophy equally well in all patients. The associated hemicranial atrophy noted in case 2 was also well depicted by both imaging techniques.

Definite cortical calcification in two patients (cases 2 and 3) was detected by CT only. In one patient (case 2), large regions of serpentine cortical calcification were noted in both frontal lobes and in the left occipitoparietal region (Figs. 2A and 2D). Only a few small foci of nonspecific hypointensity were demonstrated on T2-weighted images at the cortical-subcortical junction in these locations (Fig. 2E). In case 3, floccular calcification was seen on CT within the left occipital cortex. No evidence of hypointensity was seen on the corresponding T2-weighted images.

TABLE 1: Clinical Data in Patients with Sturge-Weber Syndrome

Case No.	Age at MR	Gender	Age at Presentation	Symptoms	Signs
1	5 mo	F	4 mo	L elementary partial seizures	R facial nevus
2	6 yr	M	2 wk	R elementary partial seizures	Bilateral facial nevi, larger on R; R hemiparesis; mental retardation
3	17 yr	M	4 yr	R elementary partial seizures; decreased vision, L eye	Bilateral facial nevi, extending to involve L neck and arm; hypertrophy of L arm; glaucoma of L eye

Note.—L = left; R = right.

TABLE 2: MR and CT Findings in Patients with Sturge-Weber Syndrome

Finding: Study	Case 1	Case 2	Case 3
Volume loss:			
MR	L > R frontal; R parietal; R occipital	L > R frontal; L parietal	L hemisphere
CT	Same	Same	Same
Hemicranial atrophy:			
MR	NS	L side	NS
CT	NS	Same	NS
Calcification:			
MR	NS	Nonspecific, hypointense foci in L frontal cortex	NS
CT	NS	Definite and extensive bifrontal, L occipital, and L parietal foci	Definite foci, L occipital
Abnormal cortex:			
MR	Hyperintense and thickened in R frontal lobe and insula	Isointense and thickened in L parietal region	NS
CT	NS	NS	NS
Abnormal white matter:			
MR	Hypointense subcortical white matter on R in frontal lobe and insula; hypointense deep white matter on R in frontal lobe and insula	Hyperintense subcortical white matter, R and L frontal and L parietal; hyperintense deep white matter, L frontal and parietal	NS
CT	NS	Less extensive hypodensity in L frontal and L parietal white matter	NS
Enlarged choroid plexus:			
MR	NS	NS	L lateral ventricle
CT	NS	NS	Same
Engorged deep veins:			
MR	NS	L > R hemisphere	L hemisphere
CT	NS	NS	NS
Miscellaneous:			
MR	Hyperintense R thalamic lesion	Cerebellar angioma	L proptosis
CT	NS	Same	Same

Note.—Signal intensities are those observed on T2-weighted images. L = left; R = right; NS = not seen.

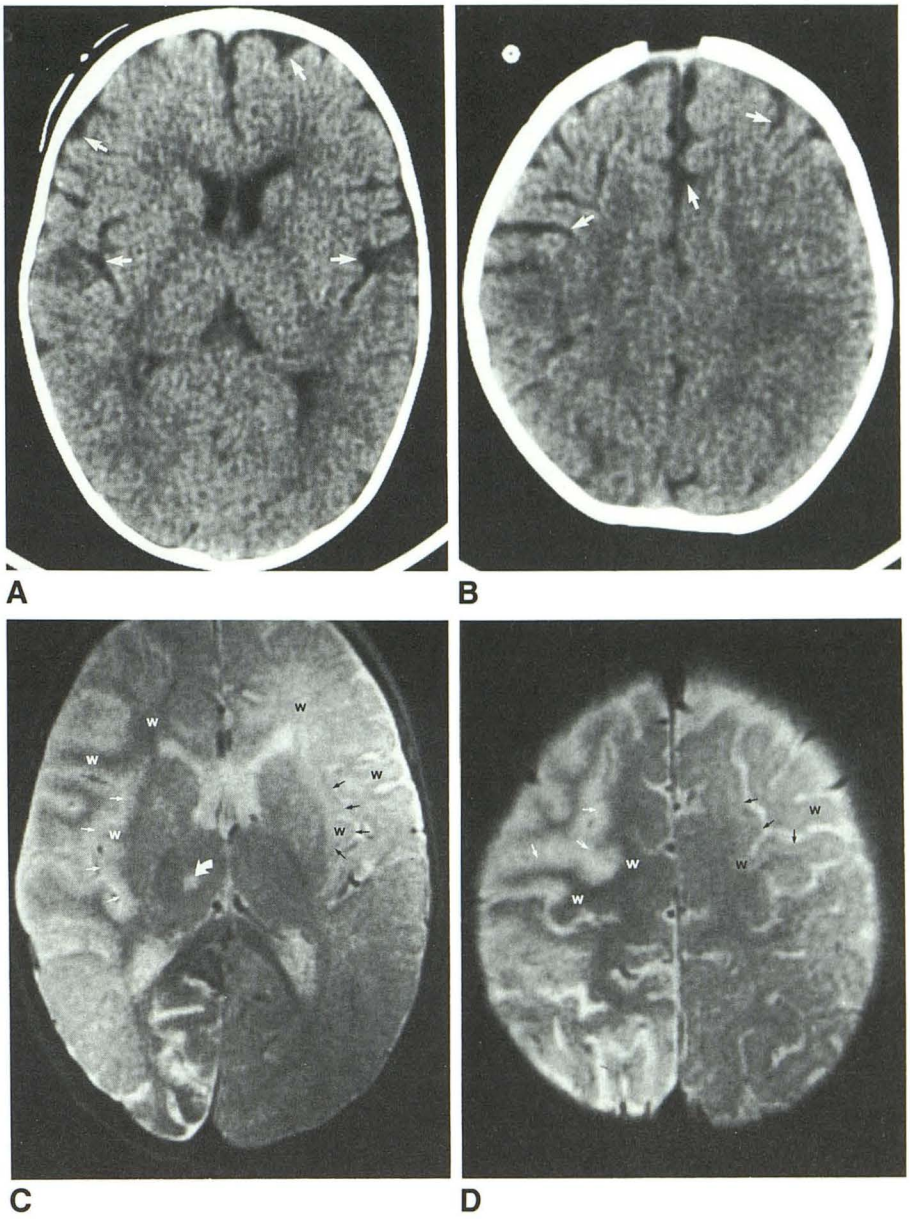

Fig. 1.—Case 1: 5-month-old girl.

***A* and *B*, Noncontrast axial CT scans show prominent sulci (*arrows*) of frontal lobes, compatible with volume loss. No abnormal gyral enhancement was seen on postcontrast CT images (not shown).**

***C* and *D*, Axial T2-weighted MR images at same levels show abnormal thickening and high signal intensity (*straight white arrows*) affecting insular cortex (*C*) and cortex of high right frontal lobe (*D*). Compare with normal cortex (*black arrows*) on left side. White matter within right forceps minor and beneath thickened cortex (*white w*) has low signal intensity, unusual in patient only 5 months old. Compare with normal white matter (*black w*) on left side. Focal lesion (*curved arrow*) is also detected within right thalamus.**

MR alone showed thickened cortex with decreased convolutions in regions of parenchymal atrophy in two patients (cases 1 and 2). T1-weighted sagittal and coronal images helped confirm the cortical thickening and decreased convolutions seen on axial T2-weighted images, especially in the high cerebral convexity regions. In the 5-month-old patient (case 1), the thickened cortex had higher signal intensity than cortex on the contralateral (asymptomatic) side on T2-weighted images. In addition, the underlying white matter had lower signal intensity than white matter on the contralateral side. These alterations resulted in a unique unilateral reversal of the normal gray-matter/white-matter signal-intensity relationship expected on T2-weighted images in a patient this age (Figs. 1C and 1D) [10]. CT in this patient showed only bilateral volume loss without abnormal cortical thickening, enhancement, or white-matter abnormality (Figs. 1A and 1B). In case 2 the thickened cortex was isointense when compared with normal cortex (Fig. 2E). Extensive regions of abnormal hyperintensity were demonstrated in the underlying white matter. The cortical thickening was not appreciated on CT in this patient (Fig. 2D). Moreover, the regions of hyperintense white matter seen on MR were more extensive than the areas of hypodense white matter shown by CT.

An abnormally large, calcified choroid plexus with intense enhancement was seen on CT in case 3 (Fig. 3A). It was ipsilateral to the cutaneous nevus. Proton-density-weighted (Fig. 3B) and T2-weighted (Fig. 3) images demonstrated equally well the increased size and signal intensity of this abnormal glomus. Prominent deep hemispheric veins in cases 2 and 3 were seen on MR only. These abnormal veins were identified by the increased caliber of their flow-dependent signal void (Figs. 2C and 3C); such engorged veins could be identified within both hemispheres in one patient (case 2). The deep veins were largest within the hemisphere most affected

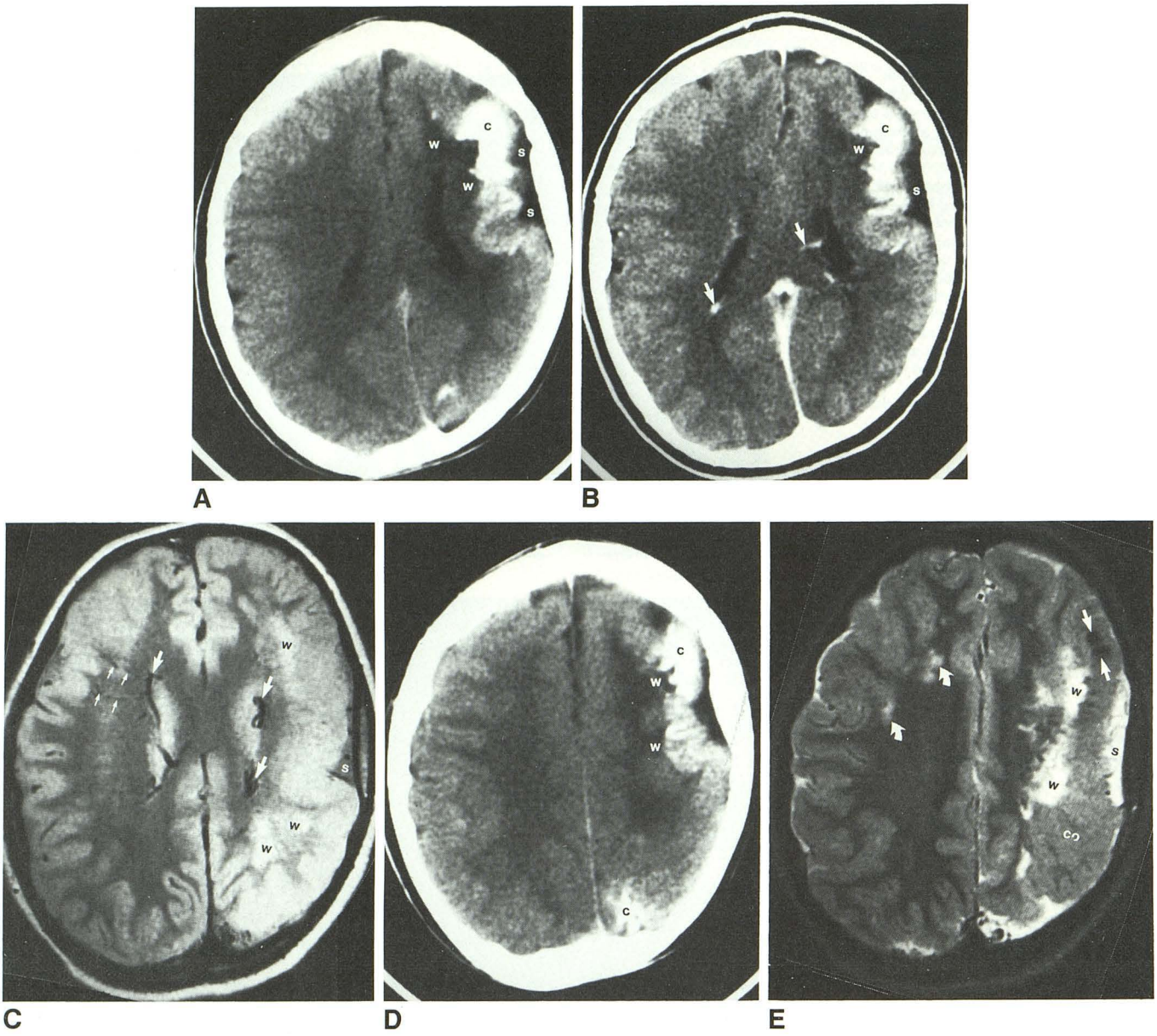

Fig. 2.—Case 2: 6-year-old boy.

***A* and *B*, Noncontrast (*A*) and postcontrast (*B*) axial CT sections show prominent subarachnoid spaces (s) overlying atrophic left frontal lobe. Cortical calcification (c) and hypodense white matter (w) of forceps minor are well shown.**

***C*, Proton-density-weighted axial MR section at same level shows high signal intensity within subcortical and periventricular white matter of left frontal and parietal lobes (w). In addition, dilated medullary veins (*small arrows*) and subependymal veins (*large arrows*, *B* and *C*) are more obvious on MR. Paucity of superficial cortical veins is seen overlying left hemisphere. No evidence of calcification is detected on MR examination at this level.**

***D*, Noncontrast CT section at a slightly higher level detects calcification (c) within left occipital and frontal cortex.**

***E*, Corresponding T2-weighted MR section. Two nonspecific foci of hypointensity measuring <5 mm in diameter (*straight arrows*) are only findings suggesting calcification. However, MR shows best thickened cortex (co) overlying left parietal lobe (compare with *D*). MR also shows abnormally high signal intensity within white matter of right frontal lobe (*curved arrows*), which appeared normal on CT (compare with *D*). Dilated subarachnoid spaces (s) and abnormal white matter (w) within left centrum semiovale are also seen.**

by parenchymal atrophy. A paucity of superficial cortical veins overlying the most affected hemisphere was seen in a single patient (case 2).

An incidental cerebellar venous angioma was noted on both postcontrast CT and MR in case 2. A curvilinear enhancing lesion was seen on CT extending within the white matter of the hemisphere perpendicular to the surface of the cerebellum. The angioma was demonstrated equally well on T2-weighted images as an abnormal curvilinear signal void. No other cerebellar abnormalities were identified in our patients.

In one patient (case 1), T2-weighted images detected a focal (<1 cm) hyperintense lesion within the thalamus (Fig. 1C). CT was completely normal in this location (Fig. 1A).

Discussion

Sturge-Weber syndrome is believed to be a sporadic disease [1, 11]. The characteristic leptomeningeal venous angioma and facial nevus in the distribution of the ophthalmic division of the trigeminal nerve are most commonly unilateral

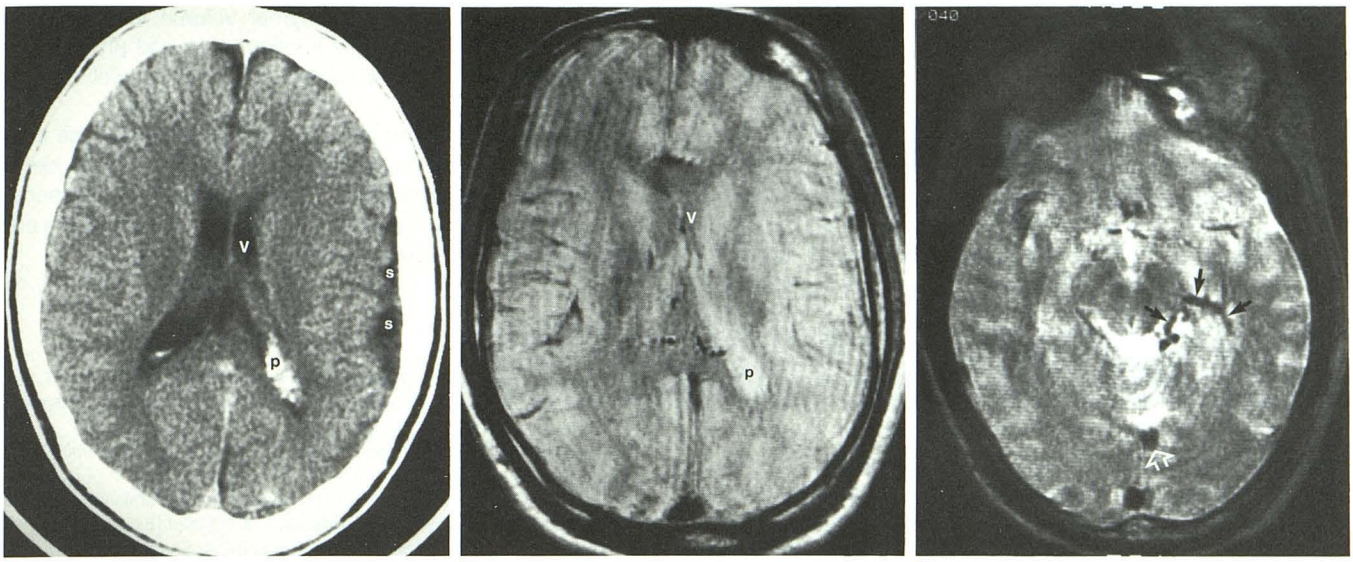

Fig. 3.—Case 3: 17-year-old boy.

***A*, Noncontrast axial CT section shows glomus of choroid plexus (p) of left lateral ventricle (v) to be enlarged and heavily calcified, suggesting angiomatous involvement. Ipsilateral subarachnoid spaces (s) are dilated, indicating cerebral atrophy.**

***B*, Proton-density-weighted image at corresponding level, although degraded by patient motion artifact, shows increased signal intensity in expected location of enlarged glomus (p).**

***C*, T2-weighted axial MR section at lower level shows engorgement of veins along medial surface of left temporal lobe (*solid arrows*) and enlargement of straight sinus (*open arrow*) compatible with shunting of blood away from veins of lateral convexity.**

but may be bilateral, as was seen in two of our patients (cases 2 and 3) [1]. The venous angioma consists of thin-walled vessels less than 150 μm in diameter that lie in the pia of the posterior parietal, temporal, and anterior occipital lobes. Parenchymal CNS atrophy accompanies the venous angioma [1]. Contralateral corporeal hemiatrophy and hemiparesis (as seen in case 2) may occur with extension of the cerebral atrophy into the motor portion of the hemisphere. Angiomatous involvement of the sclera on the same side as the facial nevus may result in glaucoma (case 3) [11]. Should the port-wine stain extend into the cutaneous vascularity of the upper extremity, there may be overgrowth of the connective tissue and underlying bone, causing hemihypertrophy (case 3).

Precise delineation of the location and extent of cerebral involvement has important prognostic implications in this disease, since bilateral or extensive involvement are often associated with more severe mental retardation and refractory seizures [1, 12, 13]. However, there have been reports of patients with bilateral parenchymal involvement who have normal intellect and an absence of seizures [14, 15].

Early CT studies described characteristic findings in patients with Sturge-Weber syndrome [4, 8, 12]. The sensitivity of noncontrast CT in the detection of the pathognomonic cortical calcification was emphasized. Parenchymal calcifications seen in Sturge-Weber syndrome occur in a pericapillary distribution in the fourth layer of the atrophied cerebral cortex and appear as curvilinear densities that follow the cerebral convolutions. The parietooccipitotemporal region is the most common site of calcification. CT often detects calcification before the age of 1 year, much earlier than is possible with skull films. Calcification was detected by CT in two of our patients aged 6 and 17 years, but not in our 5-month-old. Cerebral parenchymal atrophy may be focal or hemispheric and often is more extensive than the calcified region. Evidence of bilateral brain involvement in patients with unilateral facial nevi has been described [16]. Enhancement of the involved cortex occurs after infusion of contrast medium in most cases, but was not seen in our patients. Moderate enlargement, calcification, and enhancement of the ipsilateral choroid plexus has been described recently [7]. These findings, believed to represent angiomatous involvement [1, 7, 17] were demonstrated in our case 3.

The MR findings in this syndrome are less well defined. In one report, MR demonstrated serpentine foci of low signal in regions of very heavy parenchymal calcification [9]. The low signal was detected best on T2-weighted images, possibly because of the presence of iron in addition to calcium. MR also demonstrated dilated, tortuous deep hemispheric veins and venous thrombosis. These venous abnormalities are thought to result from compromise of superficial venous drainage and shunting of blood to the deep system as demonstrated at angiography [5, 6]. Others have reported enlarged and calcified choroid plexus lesions that were hyperintense on T2-weighted images [7]. The increased signal intensity may be related either to increased fluid (edema) content or to slow flow of venous blood [7].

In our three patients with Sturge-Weber syndrome, CT proved to be more sensitive than spin-echo MR pulse sequences in demonstrating the pathognomonic cortical calcification. In regions of calcified parenchyma, MR showed only mild, nonspecific hypointensity within some of the affected gyri. The hypointensity, when visible, was seen on heavily T2-

weighted images only. Other regions of cortical calcification were isointense relative to normal cortex. Earlier studies found that focal calcifications accompanying many parenchymal disease processes are commonly missed by MR [18]; in such instances it is likely that mobile protons in soft tissues within the interstices of the calcification generate sufficient signal to predominate over the nonmobile protons of the calcification, which generate little signal [18]. Recently, MR with gradient-echo acquisition has proved more sensitive than spin-echo MR for the detection of intraparenchymal calcification. Because the hypointensity due to calcification on gradient-echo acquisitions is nonspecific, noncontrast CT may be used to confirm its presence [19].

Thickened cortex and decreased convolutions in regions of parenchymal atrophy were detected only by MR in two of our patients. These findings have been described previously [20], and we believe they represent disturbed neuronal proliferation and migration as a consequence of abnormal cerebral venous blood flow. On T2-weighted images in a 5-month-old, thickened frontal and insular cortex was hyperintense and the underlying white matter was hypointense when compared with the normal parenchyma of the opposite, asymptomatic hemisphere. Possible explanations for the latter appearance include deposition of mineral (e.g., ferritin) in the hypointense white matter [21], accelerated myelination of the hypointense white matter [10], and technical artifacts ("shading") [22]. None of these explanations seems adequate: mineral deposition is unlikely since pathologic study confirms that calcium *and* iron deposition is confined to the cortical area of involvement in Sturge-Weber syndrome [17]; accelerated myelination is unlikely since this finding has not been documented in the syndrome [1, 10]; the "shading" artifact (commonly caused by nonuniform flip angles, coil malfunction, or insufficiently precise tuning of the shim coils) is also unlikely since this would result in a *concordant* decrease or increase in the signal intensities of affected gray *and* white matter [22]. MR and pathologic studies of Sturge-Weber patients less than 1 year old will be necessary to establish the cause of this finding.

No superficial regions of flow-related signal void, thrombosis, or other direct evidence suggested the presence of leptomeningeal angiomas in our series. Nevertheless, the paucity of superficial cortical veins and engorgement and tortuosity of subependymal and medullary veins seen in two patients provided important indirect evidence of abnormal cerebral hemodynamics. MR was most helpful in demonstrating this unusual venous drainage pattern.

The regions of abnormal signal in cortex and white-matter tracts shown by MR were more extensive than the regions of hypodense, calcified, or atrophic parenchyma revealed by CT. Moreover, MR alone demonstrated involvement of deep gray matter (thalamus) in one patient. The more extensive parenchymal abnormalities seen with MR correlate well with pathologic findings, including infarction, gliosis, and demyelination, which are known to occur in wider regions than the obviously calcified or atrophic parenchyma in Sturge-Weber syndrome [9].

In our patients, both MR and CT demonstrated equally well the morphologic changes of sulcal dilatation and ventriculomegaly accompanying parenchymal volume loss. Choroid plexus enlargement, calvarial hemiatrophy, and proptosis of a globe affected by glaucoma were also shown well by both techniques.

In conclusion, CT and MR are complementary in the evaluation of the Sturge-Weber syndrome. CT specifically identifies the pathognomonic calcification, while MR more sensitively demonstrates gray- and white-matter abnormalities and engorgement of the deep venous system.

REFERENCES

1. Alexander GL. Sturge-Weber syndrome. In: Vinken PJ, Bruyn YN, eds. *Handbook of clinical neurology*, vol. 14. *The phakomatoses.* Amsterdam: North Holland, **1972**:223–240
2. Coulam CM, Brown LR, Reese DF. Sturge-Weber syndrome. *Semin Roentgenol* **1976**;1:55–60
3. Bentson JR, Wilson GH, Newton TH. Cerebral venous drainage pattern of Sturge-Weber syndrome. *Radiology* **1971**;101:111–118
4. Makai Y, Semba A. Computed tomography of Sturge-Weber disease. *Childs Nerv Syst* **1979**;5:51–61
5. Poser GM, Taveras JM. Cerebral angiography in encephalotrigeminal angiomatosis. *Radiology* **1957**;68:327–336
6. Probst FP. Vascular morphology and angiographic flow patterns in Sturge-Weber angiomatosis: facts, thoughts and suggestions. *Neuroradiology* **1980**;20:73–78
7. Stimac GK, Solomon MA, Newton TH. CT and MRI of angiomatous malformations of the choroid plexus in patients with Sturge-Weber disease. *AJNR* **1986**;7:623–627
8. Welch K, Naheedy MH, Abroms IF, Strand RD. Computed tomography of Sturge-Weber syndrome in infants. *J Comput Assist Tomogr* **1980**;1:33–36
9. Bilaniuk LT, Zimmerman RA, Tucker S, Hackney DB, Goldberg HI, Grossman RI. MR of the Sturge-Weber syndrome (abstr). Presented at the annual meeting of the American Society of Neuroradiology, New York City, May **1987**
10. Barkovich AJ, Kjos BO, Jackson DE Jr, Norman D. Normal maturation of the neonatal and infant brain: MR imaging at 1.5-T. *Radiology* **1988**;166:173–180
11. Rosenbaum LJ. Glaucoma in Sturge-Weber's syndrome. *Birth Defects* **1982**;18:645–649
12. Verity CM, Strauss EH, Moyes PD, Wada JA, Dunn HG, Lavointe JS. Long-term follow-up after cerebral hemispherectomy: neurophysiologic, radiologic and psychological findings. *Neurology* **1982**;32:629–639
13. Gomez MR, Begin M. Seizures and mental development in patients with Sturge-Weber disease (abstr). *J Child Neurol* **1986**;1:263
14. Chaudary RR, Brudnicki A. Sturge-Weber syndrome with extensive intracranial calcifications contralateral to the bulk of the facial nevus, normal intelligence, and absent seizure disorder. *AJNR* **1987**;8:736
15. Parnitzke KH. Symptomwert und Symtomvertleilung bei der Sturge-Weberschen Krankhest. *Zentralbl Neurochir* **1956**;16:92–109
16. Boltshauser E, Wilson J, Moore RD. Sturge-Weber syndrome with bilateral intracranial calcification. *J Neurol Neurosurg Psychiatry* **1976**;39:429–435
17. Wohlwill FJ, Yakovlev PI. Histopathology of meningo-facial angiomatosis (Sturge-Weber's disease): report of four cases. *J Neuropathol Exp Neurol* **1957**;16:341–364
18. Oot RF, New PFJ, Pile-Spellman J, Rosen BR, Shoukimas GM, Davis KR. The detection of intracranial calcifications by MR. *AJNR* **1986**;7:801–809
19. Atlas SW, Grossman RI, Hackney DB, et al. Calcified intracranial lesions: detection with gradient-echo-acquisition rapid MR imaging. *AJNR* **1988**;9:253–259
20. Rao CVG, Lee SH. Cerebrovascular anomalies. In: Stark DD, Bradley WG Jr, eds. *Magnetic resonance imaging.* St. Louis: Mosby, **1988**:499–514
21. Drayer BP. Degenerative brain disorders and brain iron. In: Brant-Zawadzki M, Norman D, eds. *Magnetic resonance imaging of the central nervous system.* New York: Raven, **1987**:123–130
22. Kelly WM. Image artifacts and technical limitations. In: Brant-Zawadzki M, Norman D, eds. *Magnetic resonance imaging of the central nervous system.* New York: Raven, **1987**:43–82